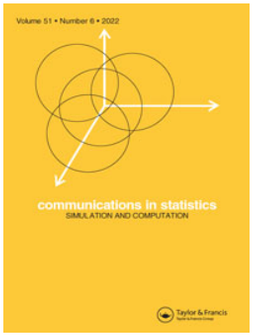

Taylor & Francis
Taylor & Francis Group

Communications in Statistics - Simulation and Computation

ISSN: 0361-0918 (Print) 1532-4141 (Online) Journal homepage: https://www.tandfonline.com/loi/lssp20

A family of density-hazard distributions for insurance losses

S. A. Abu Bakar, S. Nadarajah & N. Ngataman

To cite this article: S. A. Abu Bakar, S. Nadarajah & N. Ngataman (2020): A family of density-hazard distributions for insurance losses, Communications in Statistics - Simulation and Computation, DOI: 10.1080/03610918.2020.1784430

To link to this article: https://doi.org/10.1080/03610918.2020.1784430

COMMUNICATIONS IN STATISTICS - SIMULATION AND COMPUTATION®
https://doi.org/10.1080/03610918.2020.1784430

A family of density-hazard distributions for insurance losses

S. A. Abu Bakar[a], S. Nadarajah[b], and N. Ngataman[a]

[a]Institute of Mathematical Sciences, University of Malaya, Kuala Lumpur, Malaysia; [b]Department of Mathematics, University of Manchester, Manchester, United Kingdom

ABSTRACT

We propose a family of distributions as an alternative for a recent compound unimodal distribution for modeling insurance losses. The family of distributions, referred to as density-hazard distributions, has closed form density and distribution functions, hence easier to fit and simulate from. The distributions also show good adherence to insurance loss data and estimates risk measures relatively closely to the empirical values. In this respect, the practical use of the density-hazard distributions is demonstrated with the employment of three real insurance data including the U.S. indemnity insurance loss data, the U.S. automobile claims data, and the Norwegian fire losses data.

ARTICLE HISTORY
Received 1 July 2019
Accepted 14 June 2020

KEYWORDS
Compound unimodal distributions; Heavy tailed distributions; Insurance losses; Risk measures

1. Introduction

Model selection based on parametric distributional models can be a daunting task. A model that suits a particular data may not give best fits for others of the same kind. For this reason, the inquiry on this topic witnesses an increasing interest among researchers with newer models being proposed to substitute this curiosity.

Applications of parametric models can be found in various studies: modeling of human lifetimes (Reed 2011); prediction of pickle harvests using feedwork neural networks (Adams 1999); study of the development of breast cancer (Ardoino et al. 2012); description of the distinct dielectric properties of human tissues (Gabriel, Lau, and Gabriel 1996); estimation of the unsaturated hydraulic properties of multiphase flow in porous media (Luckner, Van Genuchten, and Nielsen 1989); design of a pragmatic cyber physical system (García-Valls, Perez-Palacin, and Mirandola 2018); modeling wind turbine power curves (Taslimi-Renani et al. 2016); analysis of the efficiency of Indian commercial banks (Silva et al. 2018); prediction of house prices (Montero, Mínguez, and Fernández-Avilés 2018); to mention a few.

In the area of insurance loss modeling, many new models have been formulated by composition of several distributions under a common structure. In this line, composite models have been developed by piecing together two distributions at a specified threshold. The models give good results when fitting insurance loss data exhibiting high frequency at the head and extreme values on the tails. A series of papers dealing with these models include among others (Cooray and Ananda 2005; Scollnik and Sun 2012; Abu Bakar et al. 2015; Calderín-Ojeda and Kwok 2016).

Mixture models for predictive modeling have also shown good indication to capture the heavy tail of insurance loss data. Mixture models are designed as a sum of weighted distributions. Bernardi, Maruotti, and Petrella (2012) considered a mixture model with skew normal components for the Danish fire insurance loss data. A Bayesian estimation method was used.

CONTACT S. Nadarajah mbbsssn2@manchester.ac.uk Department of Mathematics, University of Manchester, Manchester, United Kingdom.

Miljkovic and Grün (2016) considered mixture models with components following the Burr, gamma, inverse Burr, inverse Gaussian, and lognormal distributions and showed their flexibility in modeling the Danish fire insurance loss data. The results were further justified with three real insurance data sets as well as simulation studies (Abu Bakar, Nadarajah, and Adzhar 2018). Punzo, Mazza, and Maruotti (2018) considered a mixture model with contaminated gamma (which itself is a mixture of two unimodal gamma distributions) distributions for workers compensation data and healthcare expenditure data. Mazza and Punzo (2019) considered a mixture model with contaminated gamma or contaminated lognormal (which itself is a mixture of two unimodal lognormals) components reparameterized with respect to mode for household income data for 31 upper/middle income countries. Punzo (2019) considered a mixture model with reparameterized inverse Gaussian components for data on bodily injury claims and income of Italian households. All of the component distributions considered by these papers allow for heavy tails. Moreover, the mixture models allow for multimodality.

A new family of compound unimodal distributions has recently been introduced by Punzo, Bagnato, and Maruotti (2018). Its probability density function (PDF) takes the form

$$f(x;\theta,\gamma,\nu)=\int_0^\infty u(x;\theta,\gamma/s)w(s;\nu)ds \tag{1}$$

for $x>0$, where $u(\cdot)$ and $w(\cdot)$ are a unimodal conditional PDF and a mixing PDF, respectively. The parameter θ signifies the mode of the distribution while γ controls the concentration around the mode and ν describes tail behavior of the distribution. The compound unimodal PDF exhibits unimodal hump-shaped and positively skewed shapes. Punzo, Bagnato, and Maruotti (2018) considered nine particular cases of (1) by taking $u(\cdot)$ and $w(\cdot)$ to follow the lognormal (UL), unimodal gamma (UG) and inverse Gaussian (UIG) distributions. The model performances were assessed by means of goodness-of-fit to three real insurance data sets. Punzo, Bagnato, and Maruotti (2018) also compared the model performances to unimodal lognormal, gamma, inverse Gaussian, Weibull, loglogistic, skew-normal, and skew-t distributions. Overall, UG-LN, UG-IG, and UG-UG models were found good in terms of goodness-of-fit and in describing the empirical risk measures with respect to three insurance losses data sets.

In this article, we introduce a family of distributions referred to as the density-hazard distributions. We propose it as a substitute for the compound unimodal distribution. The distribution: has a simpler form; is easier to fit to data sets; can provide adequate fits to insurance data sets; can provide better estimation of risk measures. The set up and statistical properties of this distribution are discussed in Sec. 2. Some descriptions of the data used and model selection procedure are given in Secs. 3 and 4. Next, the model goodness-of-fit as well as application to two well-known risk measures are presented in Sec. 5. A simulation study is conducted in Sec. 6. Finally, some conclusions are outlined in Sec. 7.

2. Methodology

The density-hazard distribution attaches two distinct distributions by taking the product of a density function and a hazard rate function.

Definition. Let $g(x)$ and $h(x)$ be two PDFs both with positive support. The PDF of the density-hazard distribution is

$$f(x)=g\big(-\log\left[\bar{H}(x)\right]\big)\mu(x) \tag{2}$$

for $x>0$, where $\mu(x)=\frac{h(x)}{\bar{H}(x)}$ is a hazard rate function, $\bar{H}(x)=1-H(x)$ is a survival function and $H(x)$ is a cumulative distribution function (CDF). The CDF corresponding to (2) is

$$F(x) = G\big(-\log\big[\bar{H}(x)\big]\big) \tag{3}$$

for $x > 0$, where $G(\cdot)$ denotes the CDF corresponding to $g(\cdot)$. The corresponding quantile at probability level α, $0 \leq \alpha \leq 1$ is

$$x = H^{-1}\big\{1 - \exp\big[-G^{-1}(\alpha)\big]\big\},$$

where $G^{-1}(\cdot)$ and $H^{-1}(\cdot)$ are the quantile functions for $G(\cdot)$ and $H(\cdot)$, respectively.

By integrating (2), we obtain

$$F(x) = -\int_0^x g\big(-\log\big[\bar{H}(s)\big]\big) d\log\big[\bar{H}(s)\big].$$

(3) follows by the change-of-variable $y = -\log\big[\bar{H}(s)\big]$.

Let Y be a random variable with PDF $g(\cdot)$. Then, (2) is the PDF of X given by the transformation $Y = -\log\big[\bar{H}(X)\big]$. Note that, the logarithmic term is multiplied by -1 to ensure positivity of the resulting values since logarithmic values for probabilities are negative. It is essential to realize that the logarithmic function rearranges observations close to each other so as to properly capture extreme values at the tail.

To reduce the number of parameters involved, we take $g(\cdot)$ to be a one parameter PDF. Two parameter PDFs are considered for $h(\cdot)$. Note that this is not a mandatory requirement but as will be seen later it is sufficient for the modeling of extreme losses discussed in this article.

The exponential distribution is considered here as a choice for $g(x)$. There is no specific reason for the choice, however, the exponential distribution with a rate parameter is sufficient to scale the data used. Furthermore, it is the simplest form of distribution that allows for explicit derivation of statistical properties for the density-hazard distribution as shown below. It is well known that the PDF of an exponential distribution is

$$g(x) = \lambda \exp(-\lambda x)$$

for $x > 0$. With this choice, the PDF, CDF, and the quantile function of the density-hazard distribution become

$$f(x) = \lambda h(x) \bar{H}(x)^{\lambda - 1}, \tag{4}$$

$$F(x) = 1 - \exp\big[\lambda \log\big(\bar{H}(x)\big)\big], \tag{5}$$

and

$$F^{-1}(p) = H^{-1}\Big\{1 - (1-p)^{\frac{1}{\lambda}}\Big\}, \tag{6}$$

respectively.

Please note that it will not make sense to choose $h(x)$ to be the one parameter exponential PDF because for this choice the PDF of the density-hazard distribution will be $f(x) = \lambda g(\lambda x)$, a scaled version of the PDF g.

The distributions given by (4)–(6) will incorporate unimodality (respectively, multimodality) if h is unimodal (respectively, multimodal). Similarly, the distributions will incorporate heavy tails (respectively, light tails) if h is heavy tailed (respectively, light tailed).

We consider five choices for $h(x)$ including the lognormal, inverse Weibull, inverse Pareto, paralogistic, and inverse paralogistic PDFs. These distributions are classical and common for modeling insurance losses; see Klugman, Panjer, and Willmot (2012). The PDFs, moments and tail behaviors of the five models for the density-hazard distribution are

1. the Exponential-Lognormal (E-LN) distribution with

$$f(x) = \frac{2^{\frac{1}{2}-\lambda}\lambda e^{-\frac{[\mu-\log(x)]^2}{2\sigma^2}}\left\{\text{erf}\left[\frac{\mu-\log(x)}{\sqrt{2}\sigma}\right]+1\right\}^{\lambda-1}}{\sqrt{\pi}\sigma x},$$

$$E(X^n) = \frac{2^{\frac{1}{2}-\lambda}\lambda e^{-\frac{\mu^2}{2\sigma^2}}}{\sqrt{\pi}\sigma}\sum_{i=0}^{\infty}\binom{\lambda-1}{i}J(n,i)$$

and

$$f(x) \sim \text{const}\cdot x^{\frac{\lambda\mu}{\sigma^2}-1}(\log x)^{1-\lambda}e^{-\frac{\lambda}{2\sigma^2}(\log x)^2}$$

as $x \to \infty$, where

$$J(n,i) = \int_{-\infty}^{\infty}\exp\left[-\left(n+\frac{\mu}{\sigma^2}\right)y - \frac{y^2}{2\sigma^2}\right]\left[\text{erf}\left(\frac{\mu-y}{\sqrt{2}\sigma}\right)\right]^i dy$$

and

$$\text{erf}(x) = \frac{2}{\sqrt{\pi}}\int_0^x \exp(-t^2)dt.$$

Smaller values of λ, larger values of σ and larger values of μ lead to heavier tails. σ is also a scale parameter; μ is also a location parameter;

2. the Exponential-Inverse Weibull (E-IW) distribution with

$$f(x) = \alpha\lambda\theta^{\alpha}x^{-\alpha-1}e^{-\left(\frac{x}{\theta}\right)^{-\alpha}}\left[1-e^{-\left(\frac{x}{\theta}\right)^{-\alpha}}\right]^{\lambda-1},$$

$$E(X^n) = \lambda\theta^n\Gamma\left(1-\frac{n}{\alpha}\right)\sum_{i=0}^{\infty}\binom{\lambda-1}{i}(-1)^i(i+1)^{\frac{n}{\alpha}-1}$$

and

$$f(x) \sim \text{const}\cdot x^{-\lambda\alpha-1}$$

as $x \to \infty$, where $\Gamma(\cdot)$ denotes the gamma function defined by

$$\Gamma(a) = \int_0^{\infty} t^{a-1}e^{-t}dt.$$

Smaller values of λ and α lead to heavier tails. θ is a scale parameter;

3. the Exponential-Inverse Pareto (E-IP) distribution with

$$f(x) = \alpha\lambda\theta x^{\alpha-1}(\theta+x)^{-\alpha-1}\left[1-x^{\alpha}(\theta+x)^{-\alpha}\right]^{\lambda-1},$$

$$E(X^n) = \alpha\lambda\theta^n\sum_{i=0}^{\infty}\binom{\lambda-1}{i}(-1)^i B(1-n, n\alpha+\alpha+n)$$

and

$$f(x) \sim \text{const}\cdot x^{-\lambda-1}$$

as $x \to \infty$, where $B(\cdot,\cdot)$ denotes the beta function defined by

$$B(a,b) = \int_0^1 t^{a-1}(1-t)^{b-1}dt.$$

Smaller values of λ lead to heavier tails. θ is a scale parameter;

4. the Exponential-Paralogistic (E-PL) distribution with

$$f(x) = \alpha^2\lambda\theta^{-\alpha}x^{\alpha-1}\left[\left(\frac{x}{\theta}\right)^{\alpha}+1\right]^{-\alpha\lambda-1},$$
$$E(X^n) = \alpha\lambda\theta^n B\left(\alpha\lambda+2-\frac{n}{\alpha},\frac{n}{\alpha}+1\right)$$

and

$$f(x) \sim \text{const}\cdot x^{-\alpha^2\lambda-1}$$

as $x \to \infty$. Smaller values of λ and α lead to heavier tails. θ is a scale parameter;

5. the Exponential-Inverse Paralogistic (E-IPL) distribution with

$$f(x) = \alpha^2\lambda\theta^{\alpha}x^{-\alpha-1}\left[\left(\frac{x}{\theta}\right)^{-\alpha}+1\right]^{-\alpha-1}\left\{1-\left[\left(\frac{x}{\theta}\right)^{-\alpha}+1\right]^{-\alpha}\right\}^{\lambda-1},$$
$$E(X^n) = \alpha\lambda\theta^n\sum_{i=0}^{\infty}\binom{\lambda-1}{i}(-1)^i B\left(i\alpha+\alpha+\frac{n}{\alpha},1-\frac{n}{\alpha}\right)$$

and

$$f(x) \sim \text{const}\cdot x^{-\alpha\lambda-1}$$

as $x \to \infty$. Smaller values of λ and α lead to heavier tails. θ is a scale parameter.

The PDFs $h(x)$ corresponding to these models are given in Appendix A. The E-LN distribution has a mixture of polynomial, logarithmic, and exponential tails. The E-IW, E-IP, E-PL, and E-IPL distributions have polynomial tails. The variance, skewness, and kurtosis for the five models can be calculated using the relationships Var $(X) = E(X^2) - [E(X)]^2$, Skewness $(X) = E[X - E(X)]^3/[Var(X)]^{3/2}$, and Kurtosis $(X) = E[X - E(X)]^4/[Var(X)]^2$, respectively. Expressions for Kurtosis (X) for the E-LN, E-IW, E-IP, E-PL, and E-IPL distributions are given in Appendix B.

Note that the LN distribution is the particular case of the E-LN distribution for $\lambda = 1$; the IW distribution is the particular case of the E-IW distribution for $\lambda = 1$; the IP distribution is the particular case of the E-IP distribution for $\lambda = 1$; the PL distribution is the particular case of the E-PL distribution for $\lambda = 1$; the IPL distribution is the particular case of the E-IPL distribution for $\lambda = 1$. The likelihood ratio test will be used to check if the density-hazard distributions provide significantly better fits than their particular cases.

Plots of $f(x)$ for the five models are shown in Figure 1. We see that unimodal and monotonically decreasing shapes are possible. Larger values of λ have the effect of producing more peaked shapes. Larger values of λ also have the effect of producing longer tails.

3. Data analysis

Three sets of insurance data were used to describe appropriateness of the compound unimodal distribution in Punzo, Bagnato, and Maruotti (2018). The observation plots for the three data sets are presented in Figure 2a–c. The extreme low portion for higher values and heavy observations for small values deem classical distributions less appealing for the data. Table 1 summarizes the three data sets considered in this study. The first data set is the U.S. indemnity losses consisting of 1500 observations recorded in thousands of U.S. Dollar (USD). The data have been considered in Frees and Valdez (1998). The data can be found in the evd package of the R statistical software. The second data set contains 6773 observations due to private motor settlement claims from a U.S.-based insurer. The data can be obtained from the insurance-

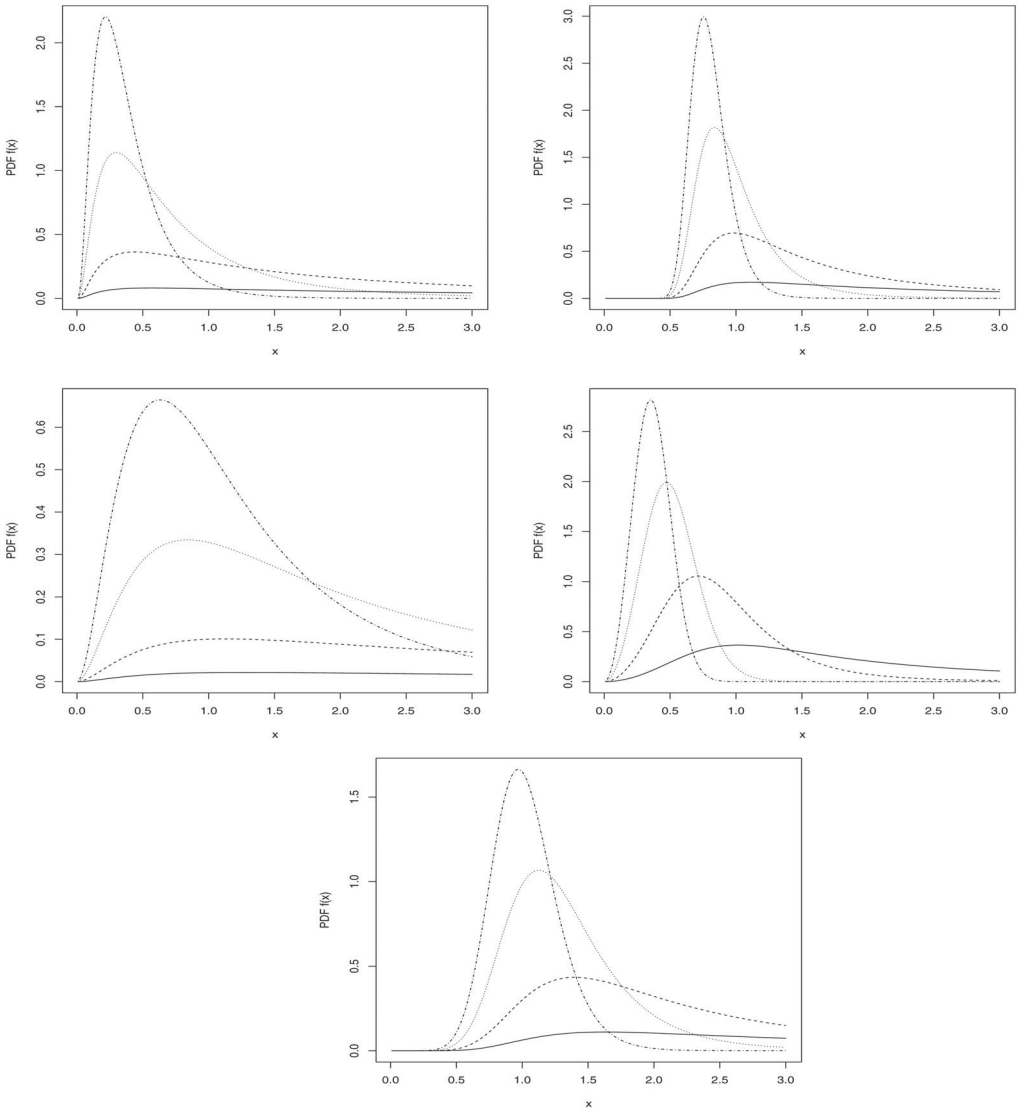

Figure 1. Plots of the PDFs of the E-LN (first row, left), E-IW (first row, right), E-IP (second row, left), E-PL (second row, right), and E-IPL (bottom) distributions. The four curves in each plot correspond to $\lambda = 0.1$ (solid curve), $\lambda = 0.5$ (curve of dashes), $\lambda = 2$ (curve of dots), and $\lambda = 5$ (curve of dots and dashes).

Data package of the R platform. Frees and Valdez (1998) showed significance of the data in a regression analysis while Bee (2017) presented an application of the data to investigate empirical appropriateness of a specific risk measure with respect to a compound Poisson-lognormal approximation. The third data set consists of 9181 observations arising from fire losses in Norway for the period between 1972 and 1992, inclusive. The data were recorded in thousands of Norwegian Krone (NKR) and can be downloaded from http://lstat.kuleuven.be/Wiley. A discussion of the Norwegian data set can be found in recent literature including Brazauskas and Kleefeld (2011), Nadarajah and Bakar (2015), and Brazauskas and Kleefeld (2016). The data were recorded with a priority of 500 thousands of NKR and thus we deducted 500 from each observation to ensure positivity of the data. Note that all these data sets represent losses related to casualty insurance.

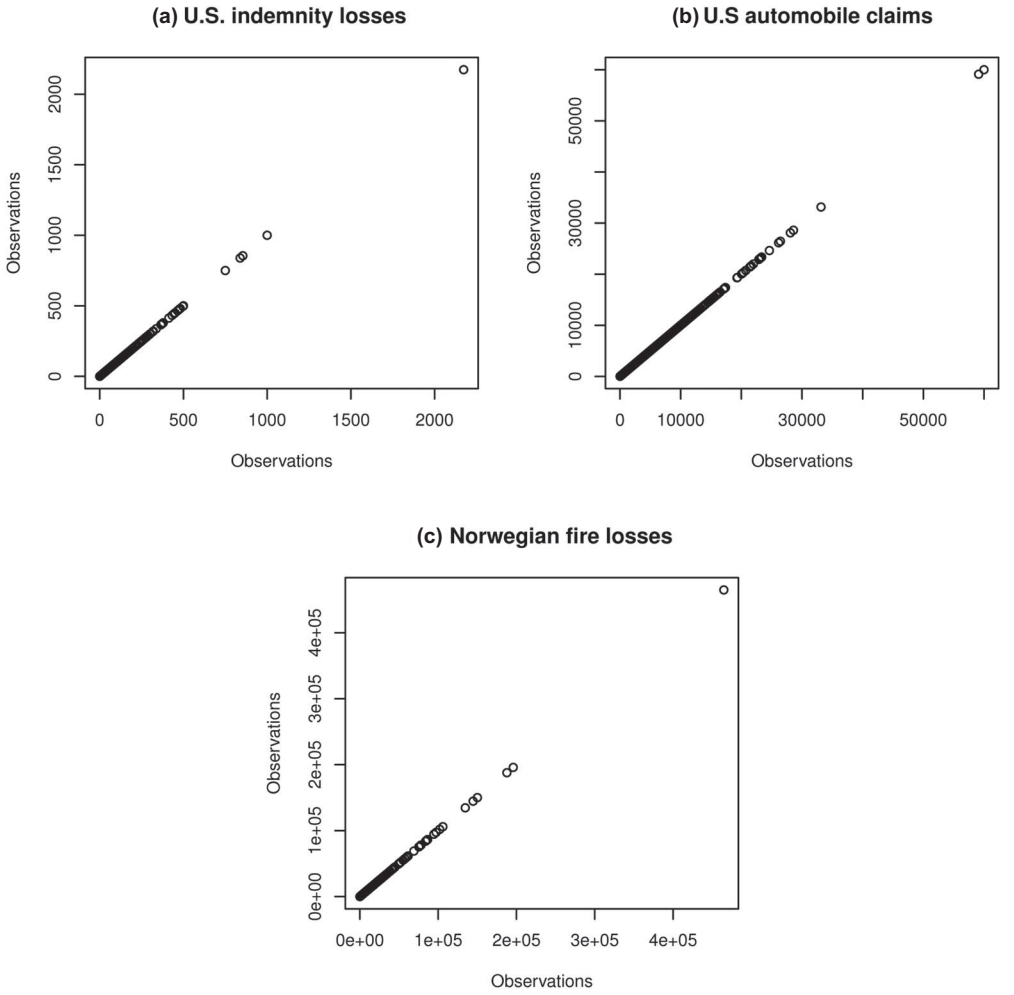

Figure 2. Observation versus observation plots for (a) U.S. indemnity losses, (b) U.S. automobile claims, and (c) Norwegian fire loss.

4. Model selection

Since the models considered consist of three parameters, it is sufficient that we compare their performance using the negative log-likelihood. As usual, a model giving a lower value of this measure will be preferred. The negative log-likelihood for the density-hazard distribution is

$$l(\boldsymbol{\theta}|x) = -\sum_{i=1}^{n} \log\left[g\{-\log\left[\bar{H}(x_i)\right]\}\right] + \sum_{i=1}^{n} \log\left[h(x_i)\right] - \sum_{i=1}^{n} \log\left[\bar{H}(x_i)\right],$$

where $\boldsymbol{\theta}$ is the set of parameters and $\mathbf{x}$ is the set of observations $x_1, x_2, ..., x_n$.

In addition, the goodness-of-fit is evaluated using the Anderson-Darling and Kolmogorov-Smirnov tests. Let $x_{(1)}, x_{(2)}, ..., x_{(N)}$ denote the ordered set of data of the original $x_1, x_2, ..., x_N$. The test statistic for the Anderson-Darling test is

$$t_{AD} = -N - \frac{1}{N}\sum_{i=1}^{N}\left\{(2i-1)\log\left[\hat{F}(x_{(i)})\right] + [2(N-i)+1]\log\left[1-\hat{F}(x_{(i)})\right]\right\}. \tag{7}$$

Table 1. Summary statistics for the U.S. indemnity losses, the U.S. automobile claims, and the Norwegian fire losses.

Statistic	U.S. indemnity losses	U.S. automobile claims	Norwegian fire losses
Total observations	1500	6773	9181
Mean	41.210	1853.035	1717.219
Minimum	0.010	9.500	0.010
Maximum	2173.595	60,000.000	464,865.000
Standard deviation	102.748	2646.909	7759.974
First quartile	4.000	523.730	200.010
Median	12.000	1001.7	520.010
Third quartile	35.000	2137.400	1300.010

On the other hand, the test statistic for the Kolmogorov-Smirnov test is

$$t_{KS} = \max(D^-, D^+), \tag{8}$$

where

$$D^- = \max_{1\le i\le N}\left\{\hat{F}(x_{(i)}) - \frac{i-1}{N}\right\} \tag{9}$$

and

$$D^+ = \max_{1\le i\le N}\left\{\frac{i}{N} - \hat{F}(x_{(i)})\right\}. \tag{10}$$

Note that $\hat{F}$ denotes the empirical CDF.

Comparison for models with different number of parameters can be made using the Bayesian Information Criterion (BIC). A lower value of the BIC suggests a preferred model over the higher value. BIC can be computed as $BIC = 2NLL + k\log n$, where NLL is the negative log-likelihood, k is the number of parameters, and n is the number of observations.

We consider two common risk measures, the Value-at-Risk (VaR) and the Conditional Tail Expectation (CTE) to show application of the proposed density-hazard distributions. If X denotes the random variable of interest, then the theoretical VaR at α probability level is

$$VaR(\alpha) = F_X^{-1}(\alpha),$$

where $F_X^{-1}(\cdot)$ denotes the inverse CDF of X. The empirical estimate is found as the quantile value at probability level α

$$VaR(\alpha) = \hat{F}_X^{-1}(\alpha),$$

where $\hat{F}_X^{-1}(\cdot)$ denotes the empirical inverse CDF. The theoretical CTE is

$$CTE(\alpha) = \frac{1}{1-\alpha}\int_\alpha^1 F_X^{-1}(s)ds.$$

Its empirical estimate is obtained as the average sum of all observations greater than the estimated VaR:

$$CTE(\alpha) = \frac{1}{w}\sum_{i=1}^{w} r_i,$$

where r_i for $i = 1, 2, \ldots, w$ are the empirical data greater than $\hat{F}_X^{-1}(\alpha)$.

In order to investigate the adherence of theoretical and empirical risk estimates, an absolute relative percentage (ARP) is employed. The ARP is simply the absolute difference between the theoretical and empirical estimates divided by the empirical one.

Table 2. Estimated values of NLL and BIC for the U.S. indemnity losses data.

Model	Number of parameters	NLL	BIC	Rank	Likelihood ratio test Statistic	p-value
IW	2	6752.176	13,518.978	13		
IP	2	6574.702	13,164.030	7		
PL	2	6572.832	13,160.290	5		
IPL	2	6573.532	13,161.690	6		
LN	2	6566.767	13,148.160	2		
E-IW	3	6565.831	13,153.602	4	372.6892	0.0000
E-IP	3	6571.483	13,164.906	8	6.4377	0.0112
E-PL	3	6572.211	13,166.362	11	1.2416	0.2652
E-IPL	3	6572.017	13,165.974	10	3.0296	0.0818
E-LN	3	6564.485	13,150.910	3	4.5638	0.0327
UG-LN	3	6558.861	13,139.662	1		
UG-UG	3	6571.902	13,165.744	9		
UG-IG	3	6585.860	13,193.660	12		

5. Results

In this section, we compare the performance of the proposed density-hazard distributions, the underlying $h(x)$ distributions, and unimodal distributions with respect to real data sets. The estimated parameters found by fitting the models to each data set are given in Table A1 of Appendix C.

5.1. U.S. indemnity data

Table 2 presents the estimated values of NLL and BIC for model selection. Due to varying number of parameters, we base our ranking of model preference on the BIC values. The UG-LN model shows the best fit followed by LN and E-LN. The least performance is shown by the IW distribution. IW, IP, PL, IPL, and LN are all nested under E-IW, E-IP, E-PL, E-IPL, and E-LN, respectively. We perform the likelihood ratio test to see if there is improvement for the latter models. All except the E-PL and E-IPL show significant improvement than their nested counterparts with respect to the U.S. indemnity data.

Table 3 reports the results with respect to risk measures between the empirical and theoretical measures. For the risk measures, the E-LN model provides better estimates of the empirical values most of the times. This can be observed for the CTE risk measure, where the E-LN model provides better estimates at the 95% and 99% levels. Overall, both models, show less than 10% of ARP between the empirical and theoretical estimates for VaR. Considering the extreme distribution of the data, the differences are of acceptable margin plus they are lower than those for the remaining models examined. In addition to the two models, the E-IW model shows good estimation of the risk measures with ARP less than 10% for all cases considered.

5.2. U.S. automobile claims data

Table 4 summarizes the estimated values of NLL and BIC for the U.S. automobile claims data. The best fit is given by UG-IG model followed by the UG-LN and E-IP. Again, the IW distribution shows the least performance. The likelihood ratio test shows significant improvement for all density-hazard distributions considered over their nested distributions.

Table 5 shows the results for the risk measures with respect to U.S. automobile insurance claims. When risk estimation is of concern, the UG-LN model does not always provide close representation of the empirical value. Two models consistently giving less than 10% of the ARP for VaR and CTE at 95% and 99% levels are the E-IW and UG-IG models.

Table 3. Estimates of Value-at-Risk (VaR) and Conditional Tail Expectation (CTE) for U.S. indemnity losses.

Model	VaR 95%	ARP	#	99%	ARP	#	CTE 95%	ARP	#	99%	ARP	#
Empirical	170.4			475.055			373.811			739.617		
IW	967.212	467.61%	13	17109.602	3501.60%	13	592714.799	158460.02%	13	10114748.551	1367465.72%	13
IP	209.462	22.92%	12	1087.958	129.02%	12	2140.394	472.59%	11	10742.587	1352.45%	11
PL	176.302	3.46%	6	776.329	63.42%	10	1734.942	364.12%	10	7334.789	891.70%	10
IPL	188.867	10.84%	10	902.564	89.99%	11	3816.171	920.88%	12	17587.385	2277.90%	12
LN	174.033	2.13%	5	531.249	11.83%	4	447.310	19.66%	4	1104.471	49.33%	5
E-IW	162.913	4.39%	8	461.515	2.85%	2	384.979	2.99%	2	901.738	21.92%	2
E-IP	169.928	0.28%	1	705.679	48.55%	9	1193.378	219.25%	9	4710.259	536.85%	9
E-PL	167.226	1.86%	4	669.233	40.87%	7	1009.217	169.98%	7	3830.891	417.96%	7
E-IPL	168.404	1.17%	3	687.477	44.72%	8	1104.307	195.42%	8	4286.397	479.54%	8
E-LN	163.534	4.03%	7	463.134	2.51%	1	383.934	2.71%	1	891.996	20.60%	1
UG-LN	168.412	1.17%	2	491.670	3.50%	3	408.079	9.17%	3	964.728	30.44%	3
UG-UG	159.283	6.52%	9	607.856	27.95%	5	697.931	86.71%	6	2357.447	218.74%	6
UG-IG	151.759	10.94%	11	333.238	29.85%	6	269.922	27.79%	5	494.565	33.13%	4

Table 4. Estimated values of NLL and BIC for the U.S. automobile claims data.

Model	Number of parameters	NLL	BIC	Rank	Likelihood ratio test Statistic	p-value
IW	2	57,985.08	115,984.793	13		
IP	2	57,536.84	115,088.298	12		
PL	2	57,204.36	114,423.344	11		
IPL	2	57,191.48	114,397.587	10		
LN	2	57,185.11	114,384.838	8		
E-IW	3	57,186.650	114,395.240	9	1596.8667	0.0000
E-IP	3	57,161.470	114,344.880	3	750.7318	0.0000
E-PL	3	57,178.080	114,378.100	6	52.5575	0.0000
E-IPL	3	57,167.470	114,356.880	4	48.0205	0.0000
E-LN	3	57,180.730	114,383.400	7	8.7511	0.0031
UG-LN	3	57,133.830	114,289.600	2		
UG-UG	3	57,175.769	114,373.478	5		
UG-IG	3	57,123.403	114,268.746	1		

Table 5. Estimates of negative log-likelihood (NLL), Value-at-Risk (VaR), and Conditional Tail Expectation (CTE) for U.S. automobile claims.

Model	VaR 95%	ARP	#	99%	ARP	#	CTE 95%	ARP	#	99%	ARP	#
Empirical	6356.726			12,052.29			10,403.811			18,172.931		
IW	18,299.454	187.88%	13	118,101.694	879.91%	13	301,334.421	2796.38%	13	1,902,836.235	10,370.72%	13
IP	15,343.260	141.37%	12	78,725.877	553.20%	12	154,655.377	1386.53%	12	775,278.811	4166.12%	12
PL	5666.895	10.85%	10	12,942.386	7.39%	5	11,361.289	9.20%	5	24,990.975	37.52%	6
IPL	7067.664	11.18%	11	21,755.788	80.51%	11	22,865.739	119.78%	11	69,121.951	280.36%	11
LN	6106.859	3.93%	6	12,670.301	5.13%	3	10,536.101	1.27%	2	19,482.709	7.21%	4
E-IW	5965.235	6.16%	8	12,171.602	0.99%	2	10,167.501	2.27%	3	18,669.560	2.73%	3
E-IP	6039.323	4.99%	7	14,258.689	18.31%	7	12,428.300	19.46%	7	27,661.611	52.21%	7
E-PL	6184.366	2.71%	3	16,863.164	39.92%	10	16,138.205	55.12%	10	43,254.380	138.02%	10
E-IPL	6110.495	3.87%	5	15,635.492	29.73%	8	14,280.397	37.26%	8	35,372.268	94.64%	8
E-LN	5957.362	6.28%	9	12,000.116	0.43%	1	9996.512	3.91%	4	18,007.479	0.91%	1
UG-LN	6253.580	1.62%	2	14,057.200	16.64%	6	11,632.873	11.81%	6	22,952.298	26.30%	5
UG-UG	6121.264	3.70%	4	16,117.551	33.73%	9	14,989.748	44.08%	9	38,406.946	111.34%	9
UG-IG	6272.222	1.33%	1	12,770.985	5.96%	4	10,514.016	1.06%	1	18,575.429	2.21%	2

5.3. Norwegian fire losses data

Table 6 summarizes the estimated value of NLL and BIC for the Norwegian fire loss data. The E-IP model gives the lowest NLL value followed by E-IPL and E-PL. All of the proposed distributions give lower NLL values than those for the best UG model (Punzo, Bagnato, and

Table 6. Estimated values of NLL and BIC for the Norwegian fire losses data.

Model	Number of parameters	NLL	BIC	Rank	Likelihood ratio test Statistic	p-value
IW	2	79,337.579	158,689.784	13		
IP	2	73,918.275	147,851.176	5		
PL	2	73,977.387	147,969.401	7		
IPL	2	74,006.675	148,027.976	8		
LN	2	753,41.823	150,698.272	12		
E-IW	3	74,624.210	149,270.360	11	9426.7376	0.0000
E-IP	3	73,704.780	147,431.500	1	426.9900	0.0000
E-PL	3	73,760.190	147,542.320	3	434.3948	0.0000
E-IPL	3	73,736.530	147,495.000	2	540.2899	0.0000
E-LN	3	74,102.740	148,227.420	9	2478.1653	0.0000
UG-LN	3	73,951.517	147924.974	6		
UG-UG	3	73,857.587	147,737.114	4		
UG-IG	3	74,114.091	148,250.122	10		

Table 7. Estimated values of negative log-likelihood (NLL), Value-at-Risk (VaR), and Conditional Tail Expectation (CTE) for Norwegian fire losses.

Model	VaR 95%	ARP	#	99%	ARP	#	CTE 95%	ARP	#	99%	ARP	#
Empirical	5889.010			19,317.410			17,890.069			50,793.358		
IW	3,008,232.599	50982.14%	13	766,233811.9	3966445.27%	13	1.15E + 14	6.42E + 09	13	2.73E + 16	5.37E + 11	13
IP	10,430.95066	77.13%	11	54,641.5639	182.86%	12	10,7608.378	501.50%	11	540,532.004	964.18%	11
PL	7572.776971	28.59%	9	33,607.00512	73.97%	9	78,144.403	336.80%	10	332,948.234	555.50%	10
IPL	10,042.30316	70.53%	10	53,595.22121	177.45%	10	110,577.437	518.09%	12	568,039.440	1018.33%	12
LN	13,043.632	121.49%	12	53,822.15192	178.62%	11	49,536.036	176.89%	9	14,9242.396	193.82%	9
E-IW	6987.483	18.65%	8	19,159.841	0.82%	1	15,617.351	12.70%	2	34,676.329	31.73%	3
E-IP	5676.419	3.61%	2	16,123.427	16.53%	3	14,711.027	17.77%	3	38,216.440	24.76%	2
E-PL	5650.7914	4.05%	5	15,321.4999	20.69%	5	13,392.168	25.14%	5	32,419.626	36.17%	5
E-IPL	5660.4884	3.88%	3	15,584.4913	19.32%	4	13,810.391	22.80%	4	34,245.430	32.58%	4
E-LN	6094.5306	3.49%	1	13,225.2612	31.54%	7	10,740.261	39.97%	7	19,593.638	61.42%	7
UG-LN	5607.252	4.78%	6	13,786.748	28.63%	6	11,306.695	36.80%	6	23,512.892	53.71%	6
UG-UG	5536.556	5.98%	7	17,624.382	8.76%	2	17,410.828	2.68%	1	50,963.141	0.33%	1
UG-IG	5654.243	3.99%	4	12,136.602	37.17%	8	9870.214	44.83%	8	17,840.886	64.88%	8

Table 8. Goodness-of-fit results.

	U.S. indemnity data		U.S. automobile claims data		Norwegian fire losses data	
Model	AD p-value	KS p-value	AD p-value	KS p-value	AD p-value	KS p-value
E-IW	0.306	0.168	0.407	0.161	0.282	0.370
E-IP	0.114	0.012	0.389	0.036	0.494	0.035
E-PL	0.118	0.014	0.114	0.030	0.268	0.039
E-IPL	0.116	0.012	0.227	0.006	0.301	0.038
E-LN	0.350	0.178	0.130	0.396	0.208	0.205
UG-LN	0.561	0.208	0.303	0.202	0.324	0.332
UG-UG	0.096	0.011	0.244	0.007	0.065	0.019
UG-IG	0.002	0.000	0.019	0.026	0.027	0.029

Maruotti 2018). Once again, IW distribution shows the least performance for model selection. All the density-hazard distributions show significant improvement over their nested models.

Table 7 reports the performance of the density-hazard distributions with respect to the Norwegian fire loss data. With regard to risk estimation, the proposed distributions provide the best fit most of the times.

5.4. Goodness-of-fit tests

The goodness-of-fit for the three data sets was evaluated using the Anderson-Darling and Kolmogorov-Smirnov tests. The results for the three data sets are shown in Table 8.

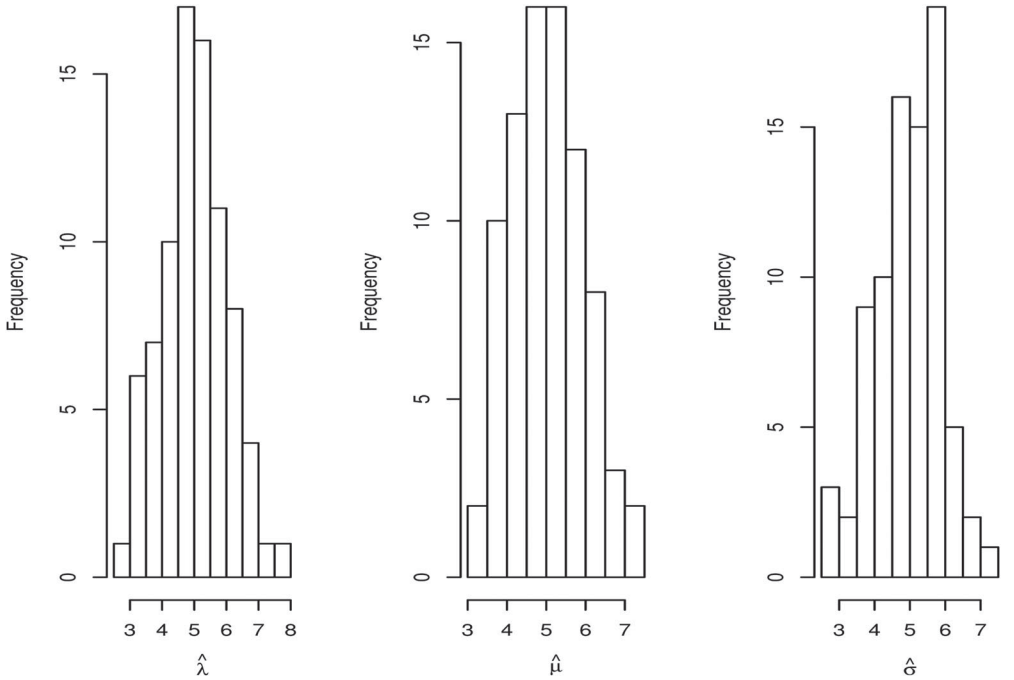

Figure 3. Histograms of parameter estimates for the 82 out of the 1000 random samples simulated from the E-LN distribution for which optim did not converge. The true parameter values were $\lambda = 5$, $\mu = 5$, and $\sigma = 5$.

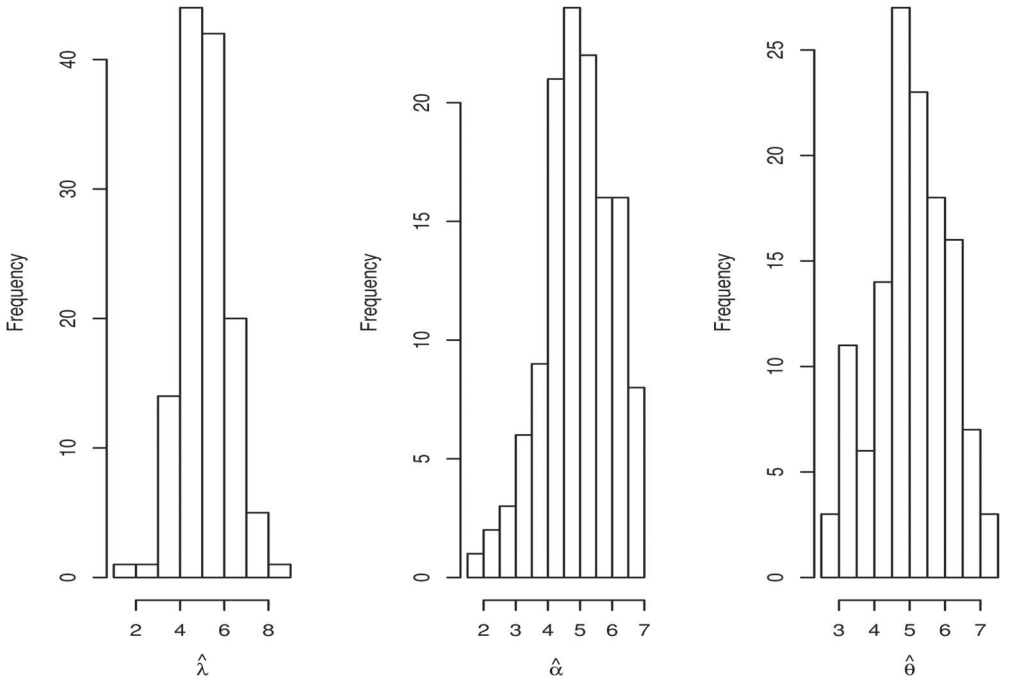

Figure 4. Histograms of parameter estimates for the 128 out of the 1000 random samples simulated from the E-IW distribution for which optim did not converge. The true parameter values were $\lambda = 5$, $\alpha = 5$, and $\theta = 5$.

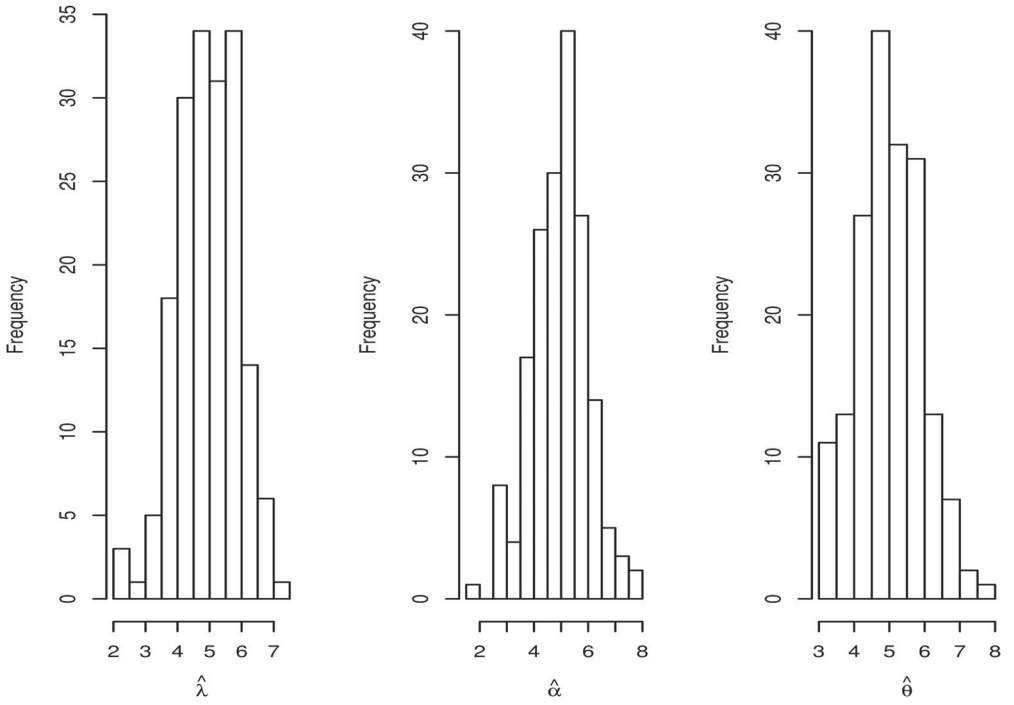

Figure 5. Histograms of parameter estimates for the 177 out of the 1000 random samples simulated from the E-IP distribution for which optim did not converge. The true parameter values were $\lambda = 5$, $\alpha = 5$, and $\theta = 5$.

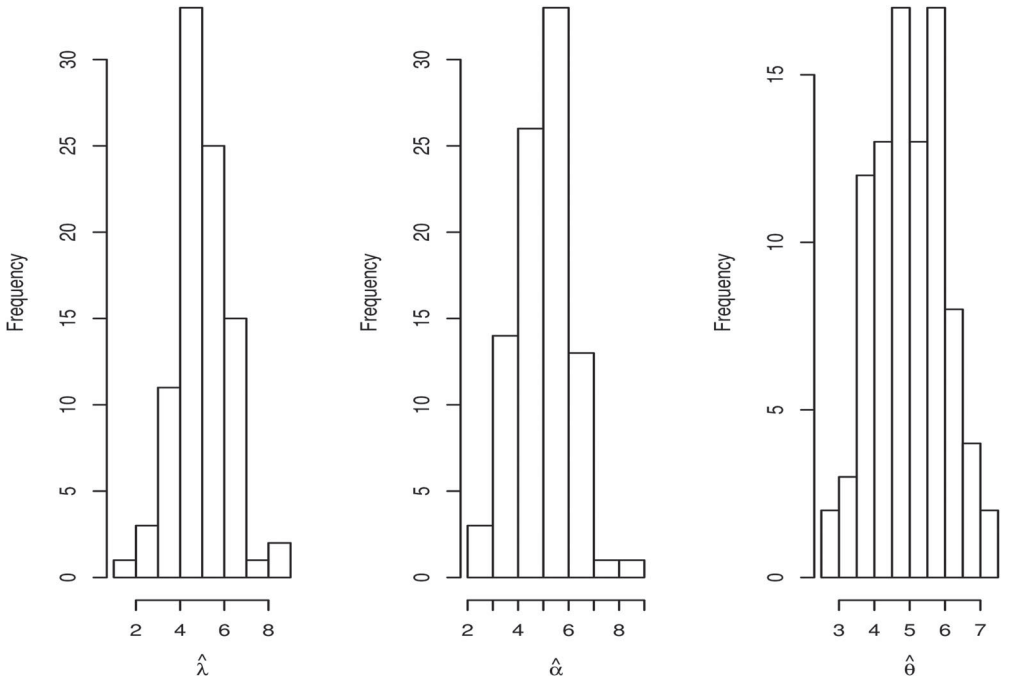

Figure 6. Histograms of parameter estimates for the 91 out of the 1000 random samples simulated from the E-PL distribution for which optim did not converge. The true parameter values were $\lambda = 5$, $\alpha = 5$, and $\theta = 5$.

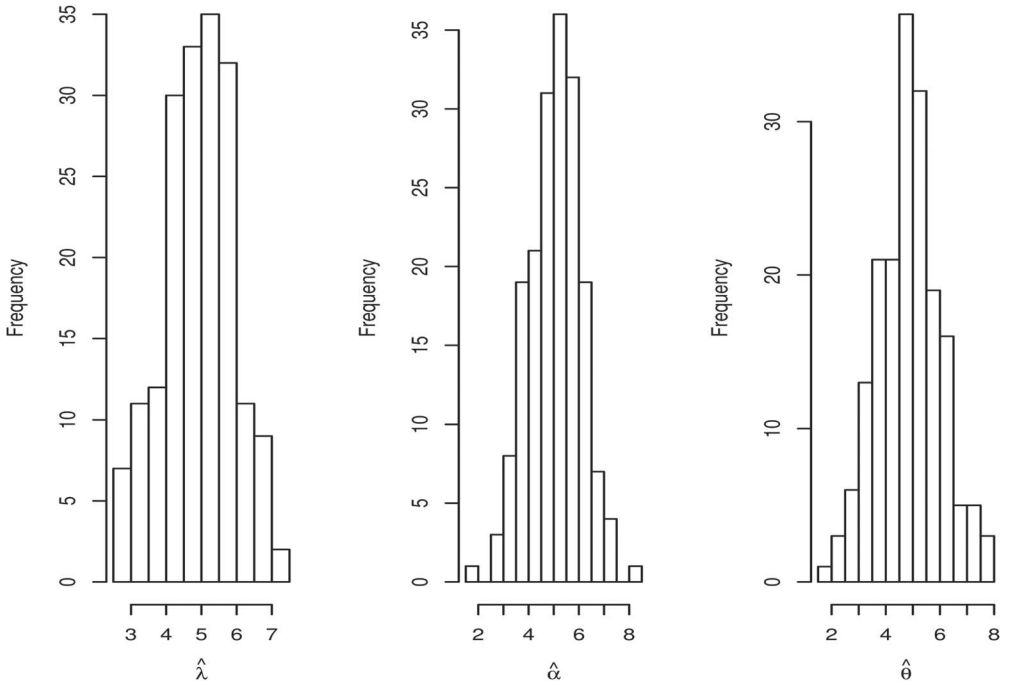

Figure 7. Histograms of parameter estimates for the 182 out of the 1000 random samples simulated from the E-IPL distribution for which optim did not converge. The true parameter values were $\lambda = 5$, $\alpha = 5$, and $\theta = 5$.

We see that all of the proposed distributions give adequate fits with respect to the Anderson-Darling test. Two of the proposed distributions give adequate fits with respect to the Kolmogorov-Smirnov test. Only two of the unimodal models give adequate fits with respect to the Anderson-Darling test and one of the unimodal models gives adequate fits with respect to the Kolmogorov-Smirnov test.

6. A simulation study

The computations for this article were carried out in R (R Core Team 2019). The optimization was performed using the optim function in R. We employ an intensive initialization procedure for each model. For example, for the E-LN model, the initial values were chosen to correspond to all combinations of

- $\lambda = 1, 2, \ldots, 10$;
- $\mu = -5, -4, \ldots, 5$;
- $\sigma = 1, 2, \ldots, 10$.

The function optim was executed for each combination. Whenever the function converged, the estimates returned were the same (Abu Bakar and Nadarajah 2019). The R codes for these computation can be provided upon request from the authors.

The validity of the statement is illustrated in Figures 3–7 by a simulation study. For at least 800 of the simulated samples, the parameter estimates were the same as the true parameter values, each corresponding to convergence of optim. For other samples, optim did not converge and the parameter estimates were not the same as the true parameter values. We have considered all

five of the density-hazard distributions and selected parameter values for each. The results were similar for a wide range of other parameter values.

7. Conclusions

The density-hazard distributions are flexible distributions based on a combination of two distinct distributions. Expressions for many statistical properties of the model are in closed form allowing for analytic examination and computational encryption.

We considered five density-hazard distributions and compared them to the three best fitted models in (Punzo, Bagnato, and Maruotti 2018). In terms of goodness-of-fit, the proposed distributions show better performance than the compound unimodal model with respect to Norwegian fire claim data. They perform slightly better for the U.S. indemnity loss data and the U.S. automobile claim data. With respect to risk estimation, there is no single model that works better. Conclusions were made based on absolute relative differences between the theoretical and empirical measures. At least one of the proposed distributions provides a competitive alternative to the best compound unimodal model for each data considered.

As a note for caution, conclusions on model performance solely on the goodness-of-fit can be misleading when risk measurements are of concern. In this respect, we are in agreement to the conclusions in Calderín-Ojeda (2018) that actuarial judgment and experience have a central role in decision making process.

There are vast opportunities to extend the research as the study only makes use of the exponential distribution as the principal model. Besides, consistency between goodness-of fit and risk measures can be given a second thought. In this respect, a more reliable connection between the two can be an interesting topic of research.

Appendix A

The PDFs $h(x)$ corresponding to the five density-hazard distributions are

(i) the Lognormal (E-LN) distribution with PDF

$$h(x) = \frac{1}{\sqrt{\pi}\sigma x} e^{-\frac{[\mu - \log(x)]^2}{2\sigma^2}};$$

(ii) the Inverse Weibull (E-IW) distribution with PDF

$$h(x) = \frac{\alpha\theta^{\alpha}}{x^{\alpha+1}} e^{\left(\frac{x}{\theta}\right)^{-\alpha}};$$

(iii) the Inverse Pareto (E-IP) distribution with PDF

$$h(x) = \frac{\alpha\theta}{(x+\theta)^2}\left(\frac{x}{x+\theta}\right)^{\alpha-1};$$

(iv) the Paralogistic (E-PL) distribution with PDF

$$h(x) = \frac{\alpha^2 x^{\alpha-1}}{\theta^{\alpha}}\left[\left(\frac{x}{\theta}\right)^{\alpha} + 1\right]^{-\alpha-1};$$

(v) the Inverse Paralogistic (E-IPL) distribution with PDF

$$h(x) = \frac{\alpha^2\theta^{\alpha}}{x^{\alpha+1}}\left[\left(\frac{x}{\theta}\right)^{-\alpha} + 1\right]^{-\alpha-1}.$$

Appendix B

Expressions for Kurtosis (X) for the E-LN, E-IW, E-IP, E-PL, and E-IPL distributions are

$$\left\{\frac{\pi^{3/2}\sigma^3}{2^{\frac{3}{2}-3\lambda}\lambda^3 e^{-\frac{3\mu^2}{2\sigma^2}}}\sum_{i=0}^{\infty}\binom{\lambda-1}{i}J(4,i)\right.$$
$$-\frac{2\pi\sigma^2}{2^{-2\lambda}\lambda^2 e^{-\frac{\mu^2}{\sigma^2}}}\left[\sum_{i=0}^{\infty}\binom{\lambda-1}{i}J(3,i)\right]\left[\sum_{i=0}^{\infty}\binom{\lambda-1}{i}J(1,i)\right]$$
$$+\frac{6\pi^{1/2}\sigma}{2^{\frac{1}{2}-\lambda}\lambda e^{-\frac{\mu^2}{2\sigma^2}}}\left[\sum_{i=0}^{\infty}\binom{\lambda-1}{i}J(2,i)\right]\left[\sum_{i=0}^{\infty}\binom{\lambda-1}{i}J(1,i)\right]^2$$
$$\left.-3\left[\sum_{i=0}^{\infty}\binom{\lambda-1}{i}J(1,i)\right]^4\right\}$$
$$\Bigg/\left\{\frac{\pi^{1/2}\sigma}{2^{\frac{1}{2}-\lambda}\lambda e^{-\frac{\mu^2}{2\sigma^2}}}\left[\sum_{i=0}^{\infty}\binom{\lambda-1}{i}J(2,i)\right]-\left[\sum_{i=0}^{\infty}\binom{\lambda-1}{i}J(1,i)\right]^2\right\}^2,$$

$$\left\{\lambda^{-3}\Gamma\left(1-\frac{4}{\alpha}\right)\sum_{i=0}^{\infty}\binom{\lambda-1}{i}(-1)^i(i+1)^{\frac{4}{\alpha}-1}\right.$$
$$-4\lambda^{-2}\Gamma\left(1-\frac{1}{\alpha}\right)\Gamma\left(1-\frac{3}{\alpha}\right)\left[\sum_{i=0}^{\infty}\binom{\lambda-1}{i}(-1)^i(i+1)^{\frac{1}{\alpha}-1}\right]\left[\sum_{i=0}^{\infty}\binom{\lambda-1}{i}(-1)^i(i+1)^{\frac{3}{\alpha}-1}\right]$$
$$+6\lambda^{-1}\Gamma^2\left(1-\frac{1}{\alpha}\right)\Gamma\left(1-\frac{2}{\alpha}\right)\left[\sum_{i=0}^{\infty}\binom{\lambda-1}{i}(-1)^i(i+1)^{\frac{1}{\alpha}-1}\right]^2\left[\sum_{i=0}^{\infty}\binom{\lambda-1}{i}(-1)^i(i+1)^{\frac{2}{\alpha}-1}\right]$$
$$\left.-3\Gamma^4\left(1-\frac{1}{\alpha}\right)\left[\sum_{i=0}^{\infty}\binom{\lambda-1}{i}(-1)^i(i+1)^{\frac{1}{\alpha}-1}\right]^4\right\}$$
$$\Bigg/\left\{\lambda^{-1}\Gamma\left(1-\frac{2}{\alpha}\right)\left[\sum_{i=0}^{\infty}\binom{\lambda-1}{i}(-1)^i(i+1)^{\frac{2}{\alpha}-1}\right]\right.$$
$$\left.-\Gamma^2\left(1-\frac{1}{\alpha}\right)\left[\sum_{i=0}^{\infty}\binom{\lambda-1}{i}(-1)^i(i+1)^{\frac{1}{\alpha}-1}\right]^2\right\}^2,$$

$$\left\{(\alpha\lambda)^{-3}\sum_{i=0}^{\infty}\binom{\lambda-1}{i}(-1)^i B(-3,4\alpha+\alpha+4)\right.$$
$$-4(\alpha\lambda)^{-2}\left[\sum_{i=0}^{\infty}\binom{\lambda-1}{i}(-1)^i B(-2,3\alpha+\alpha+3)\right]\left[\sum_{i=0}^{\infty}\binom{\lambda-1}{i}(-1)^i B(0,\alpha+\alpha+1)\right]$$
$$+6(\alpha\lambda)^{-1}\left[\sum_{i=0}^{\infty}\binom{\lambda-1}{i}(-1)^i B(-1,2\alpha+\alpha+2)\right]\left[\sum_{i=0}^{\infty}\binom{\lambda-1}{i}(-1)^i B(0,\alpha+\alpha+1)\right]^2$$
$$\left.-3\left[\sum_{i=0}^{\infty}\binom{\lambda-1}{i}(-1)^i B(0,\alpha+\alpha+1)\right]^4\right\}$$
$$\Bigg/\left\{(\alpha\lambda)^{-1}\left[\sum_{i=0}^{\infty}\binom{\lambda-1}{i}(-1)^i B(-1,2\alpha+\alpha+2)\right]\right.$$
$$\left.-\left[\sum_{i=0}^{\infty}\binom{\lambda-1}{i}(-1)^i B(0,\alpha+\alpha+1)\right]^2\right\}^2,$$

$$\left\{(\alpha\lambda)^{-3}B\left(\alpha\lambda+2-\frac{4}{\alpha},\frac{4}{\alpha}+1\right)\right.$$
$$-4(\alpha\lambda)^{-2}B\left(\alpha\lambda+2-\frac{3}{\alpha},\frac{3}{\alpha}+1\right)B\left(\alpha\lambda+2-\frac{1}{\alpha},\frac{1}{\alpha}+1\right)$$
$$+6(\alpha\lambda)^{-1}B\left(\alpha\lambda+2-\frac{2}{\alpha},\frac{2}{\alpha}+1\right)B^2\left(\alpha\lambda+2-\frac{1}{\alpha},\frac{1}{\alpha}+1\right)$$
$$\left.-3B^4\left(\alpha\lambda+2-\frac{1}{\alpha},\frac{1}{\alpha}+1\right)\right\}$$
$$\Big/\left\{(\alpha\lambda)^{-1}B\left(\alpha\lambda+2-\frac{2}{\alpha},\frac{2}{\alpha}+1\right)-B^2\left(\alpha\lambda+2-\frac{1}{\alpha},\frac{1}{\alpha}+1\right)\right\}^2$$

and

$$\left\{(\alpha\lambda)^{-3}\sum_{i=0}^{\infty}\binom{\lambda-1}{i}(-1)^iB\left(i\alpha+\alpha+\frac{4}{\alpha},1-\frac{4}{\alpha}\right)\right.$$
$$-4(\alpha\lambda)^{-2}\left[\sum_{i=0}^{\infty}\binom{\lambda-1}{i}(-1)^iB\left(i\alpha+\alpha+\frac{3}{\alpha},1-\frac{3}{\alpha}\right)\right]\left[\sum_{i=0}^{\infty}\binom{\lambda-1}{i}(-1)^iB\left(i\alpha+\alpha+\frac{1}{\alpha},1-\frac{1}{\alpha}\right)\right]$$
$$+6(\alpha\lambda)^{-1}\left[\sum_{i=0}^{\infty}\binom{\lambda-1}{i}(-1)^iB\left(i\alpha+\alpha+\frac{2}{\alpha},1-\frac{2}{\alpha}\right)\right]\left[\sum_{i=0}^{\infty}\binom{\lambda-1}{i}(-1)^iB\left(i\alpha+\alpha+\frac{1}{\alpha},1-\frac{1}{\alpha}\right)\right]^2$$
$$\left.-3\left[\sum_{i=0}^{\infty}\binom{\lambda-1}{i}(-1)^iB\left(i\alpha+\alpha+\frac{1}{\alpha},1-\frac{1}{\alpha}\right)\right]^4\right\}$$
$$\Big/\left\{(\alpha\lambda)^{-1}\left[\sum_{i=0}^{\infty}\binom{\lambda-1}{i}(-1)^iB\left(i\alpha+\alpha+\frac{2}{\alpha},1-\frac{2}{\alpha}\right)\right]\right.$$
$$\left.-\left[\sum_{i=0}^{\infty}\binom{\lambda-1}{i}(-1)^iB\left(i\alpha+\alpha+\frac{1}{\alpha},1-\frac{1}{\alpha}\right)\right]^2\right\}^2,$$

respectively.

Appendix C

The estimated parameters of the five density-hazard distributions for the U.S. indemnity losses, U.S. automobile claims, and Norwegian fire losses are given below.

Table A1. Estimated parameters of the density-hazard distributions for the U.S. indemnity loss, U.S. automobile claims, and Norwegian fire losses data.

Models	Parameters	Estimated parameters U.S. indemnity losses	U.S. automobile claims	Norwegian fire losses
E-IW	λ	25.692381	18.528012	8.799866
	α	0.191764	0.319983	0.194216
	θ	10,104.855513	44,473.527493	43019.817210
E-IP	λ	1.179710	2.167918	1.801065
	α	1.079268	2.133457	0.765321
	θ	13.448357	876.637687	1793.378456
E-PL	λ	1.186777	0.589634	3.008908
	α	1.012365	1.669387	0.831867
	θ	15.511115	1028.602827	2065.734051
E-IPL	λ	1.174263	1.333596	2.195108
	α	1.017483	1.357869	0.896040
	θ	14.601457	1001.718352	1978.291315
E-LN	λ	1.888748	1.463452	2251.629756
	μ	3.484776	7.342285	26.191545
	σ	1.954556	1.194178	5.816519

Acknowledgment

The authors would like to thank the Editor and the two referees for careful reading and comments which greatly improved the paper.

Funding

This work has been supported by the Ministry of Higher Education, Malaysia under Fundamental Research Grant Scheme (FRGS) FP040-2017A.

References

Abu Bakar, S. A., N. A. Hamzah, M. Maghsoudi, and S. Nadarajah. 2015. Modeling loss data using composite models. *Insurance: Mathematics and Economics* 61:146–54. doi:10.1016/j.insmatheco.2014.08.008.

Abu Bakar, S. A., and S. Nadarajah. 2019. Risk measure estimation under two component mixture models with trimmed data. *Journal of Applied Statistics* 46 (5):835–52. doi:10.1080/02664763.2018.1517146.

Abu Bakar, S. A., S. Nadarajah, and Z. A. Adzhar. 2018. Loss modeling using Burr mixtures. *Empirical Economics* 54 (4):1503–16. doi:10.1007/s00181-017-1269-7.

Adams, J. B. 1999. Predicting pickle harvests using a parametric feedforward neural network. *Journal of Applied Statistics* 26 (2):165–76. doi:10.1080/02664769922502.

Ardoino, I., E. M. Biganzoli, C. Bajdik, P. J. Lisboa, P. Boracchi, and F. Ambrogi. 2012. Flexible parametric modelling of the hazard function in breast cancer studies. *Journal of Applied Statistics* 39 (7):1409–21. doi:10.1080/02664763.2011.650685.

Bee, M. 2017. Density approximations and var computation for compound Poisson-lognormal distributions. *Communications in Statistics - Simulation and Computation* 46 (3):1825–41. doi:10.1080/03610918.2015.1016237.

Bernardi, M., A. Maruotti, and L. Petrella. 2012. Skew mixture models for loss distributions: A Bayesian approach. *Insurance: Mathematics and Economics* 51 (3):617–23. doi:10.1016/j.insmatheco.2012.08.002.

Brazauskas, V., and A. Kleefeld. 2011. Folded and log-folded-t distributions as models for insurance loss data. *Scandinavian Actuarial Journal* 2011 (1):59–74. doi:10.1080/03461230903424199.

Brazauskas, V., and A. Kleefeld. 2016. Modeling severity and measuring tail risk of Norwegian fire claims. *North American Actuarial Journal* 20 (1):1–16. doi:10.1080/10920277.2015.1062784.

Calderín-Ojeda, E. 2018. A note on parameter estimation in the composite Weibull-Pareto distribution. *Risks* 6 (1):1–8. doi:10.3390/risks6010011.

Calderín-Ojeda, E., and C. F. Kwok. 2016. Modeling claims data with composite Stoppa models. *Scandinavian Actuarial Journal* 2016 (9):817–36. doi:10.1080/03461238.2015.1034763.

Cooray, K., and M. A. Ananda. 2005. Modeling actuarial data with a composite lognormal-Pareto model. *Scandinavian Actuarial Journal* 2005 (5):321–34. doi:10.1080/03461230510009763.

Core Team, R. 2019. *R: A Language and Environment for Statistical Computing. R Foundation for Statistical Computing*, Vienna, Austria,

Frees, E. W., and E. A. Valdez. 1998. Understanding relationships using copulas. *North American Actuarial Journal* 2 (1):1–25. doi:10.1080/10920277.1998.10595667.

Gabriel, S., R. W. Lau, and C. Gabriel. 1996. The dielectric properties of biological tissues: III. Parametric models for the dielectric spectrum of tissues. *Physics in Medicine and Biology* 41 (11):2271–93. doi:10.1088/0031-9155/41/11/003.

García-Valls, M., D. Perez-Palacin, and R. Mirandola. 2018. Pragmatic cyber-physical systems design based on parametric models. *Journal of Systems and Software* 144:559–72. doi:10.1016/j.jss.2018.06.044.

Klugman, S. A., H. H. Panjer, and G. E. Willmot. 2012. *Loss models: From data to decisions*. Vol. 715. John Wiley and Sons.

Luckner, L., M. Van Genuchten, and D. R. Nielsen. 1989. A consistent set of parametric models for the two-phase flow of immiscible fluids in the subsurface. *Water Resources Research* 25 (10):2187–93. doi:10.1029/WR025i010p02187.

Mazza, A., and A. Punzo. 2019. Modeling household income with contaminated unimodal distributions. In *New statistical developments in data science, Springer Proceedings in Mathematics and Statistics*, ed. A. Petrucci, F. Racioppi, and R. Verde, 373–91. Vol. 288. Springer.

Miljkovic, T., and B. Grün. 2016. Modeling loss data using mixtures of distributions. *Insurance: Mathematics and Economics* 70:387–96. doi:10.1016/j.insmatheco.2016.06.019.

Montero, J. M., R. Mínguez, and G. Fernández-Avilés. 2018. Housing price prediction: Parametric versus semi-parametric spatial hedonic models. *Journal of Geographical Systems* 20 (1):27–55. doi:10.1007/s10109-017-0257-y.

Nadarajah, S., and S. A. A. Bakar. 2015. New folded models for the log-transformed Norwegian fire claim data. *Communications in Statistics - Theory and Methods* 44 (20):4408–40. doi:10.1080/03610926.2013.793348.

Punzo, A. 2019. A new look at the inverse Gaussian distribution with applications to insurance and economic data. *Journal of Applied Statistics* 46 (7):1260–87. doi:10.1080/02664763.2018.1542668.

Punzo, A., L. Bagnato, and A. Maruotti. 2018. Compound unimodal distributions for insurance losses. *Insurance: Mathematics and Economics* 81:95–107. doi:10.1016/j.insmatheco.2017.10.007.

Punzo, A., A. Mazza, and A. Maruotti. 2018. Fitting insurance and economic data with outliers: A flexible approach based on finite mixtures of contaminated gamma distributions. *Journal of Applied Statistics* 45 (14): 2563–84. doi:10.1080/02664763.2018.1428288.

Reed, W. J. 2011. A flexible parametric survival model which allows a bathtub-shaped hazard rate function. *Journal of Applied Statistics* 38 (8):1665–80. doi:10.1080/02664763.2010.516388.

Scollnik, D., and C. Sun. 2012. Modeling with Weibull-Pareto models. *North American Actuarial Journal* 16 (2): 260–72. doi:10.1080/10920277.2012.10590640.

Silva, T. C., B. M. Tabak, D. O. Cajueiro, and M. V. B. Dias. 2018. Adequacy of deterministic and parametric frontiers to analyze the efficiency of Indian commercial banks. *Physica A: Statistical Mechanics and Its Applications* 506:1016–25. doi:10.1016/j.physa.2018.04.100.

Taslimi-Renani, E., M. Modiri-Delshad, M. F. M. Elias, and N. A. Rahim. 2016. Development of an enhanced parametric model for wind turbine power curve. *Applied Energy* 177:544–52. doi:10.1016/j.apenergy.2016.05.124.